THE POSITIONS AND MOVEMENTS OF THE SOURCES OF SOLAR RADIO BURSTS OF SPECTRAL TYPE II

By A. A. Weiss*

[*Manuscript received January* 24, 1963]

Summary

The east-west position coordinates of the sources of 22 type II radio bursts, measured in the range 40–70 Mc/s using a swept-frequency interferometer, are analysed and discussed, in conjunction with dynamic spectra obtained in the frequency range 15–210 Mc/s. Many bursts are multiple and consist of a number of separate bursts excited by disturbances ejected in different directions from the vicinity of an optical flare, which may be equally complex.

A statistical analysis of position data for type II and type III bursts, which reveals a remarkable similarity in the general behaviour of the two types of bursts, confirms the hypothesis of generation of the radio emissions by plasma oscillations. Other topics discussed are the relative intensities of fundamental and second harmonic bands of the same burst, the relative positions of the sources of fundamental and second harmonic bands of identical frequency, and the relative positions of the sources of the two ridges of a split band.

Many type II bursts exhibit temporal changes of position at a single frequency. These are indicative of tangential movements in the solar atmosphere, with speeds of the order of 1000–2000 km/s. The spectra of these bursts with movement on the disk are characterized by little or no drift of frequency with time, and by broad bandwidth.

A mean radial distribution of electron density in the disturbed corona is derived. This distribution does not differ greatly from that found optically for the average coronal streamer.

I. Introduction

The type II, slow-drift, radio burst is an intense narrow-band component of the metre wavelength radio emission which may accompany solar flares. Bursts of this type have the characteristics of a drift of some of the main spectral features from high to low frequencies at rates of up to 1 Mc/s per second, emission at fundamental and second harmonic frequencies, and a duration of the order of minutes (Roberts 1959). It is believed that the frequency drift is due to the excitation, in the coronal gas, of plasma oscillations whose frequency decreases with time as an exciting agency moves out through regions of decreasing electron density. The velocities of the exciting agencies, inferred from these drift rates, are uncertain because of lack of knowledge of the electron density distribution in the corona. They are currently estimated to be 1000–1500 km/s. The exciting agency is probably a magneto-hydrodynamic shock front, driven by a cloud of ions and electrons ejected from a flare (Wild 1962). If this *plasma hypothesis* is correct, we would expect type II bursts to exhibit positions which may be independent of time at a single frequency but which show a systematic variation with frequency. Preliminary verification of the

* Division of Radiophysics, C.S.I.R.O., University Grounds, Chippendale, N.S.W.

hypothesis has been given by Wild, Sheridan, and Trent (1959), on the basis of two type II bursts observed with a swept-frequency interferometer capable of measuring the east-west coordinate of the position of the source as a function of both time and frequency.

In the present paper this prediction is submitted to a more searching test, using positions measured with the same instrument, over the frequency range 40–70 Mc/s, for 22 type II events recorded from June 1958 to December 1961. Another major topic discussed is the tangential movement apparently shown by the sources of some of these bursts.

The complexity of type II bursts, evident from the most casual inspection of the dynamic spectra, is apparent also in the position data. The recognition and interpretation of this complexity, which usually takes the form of abrupt changes in position during the development of a burst, were greatly helped and indeed in some cases only made possible by the availability of a dynamic spectrum for each of the events studied. The spectra were obtained with the Dapto solar radio spectrograph. Over the whole of the period for which positions have been measured the upper frequency limit of the spectra is 210 Mc/s. The lower limit has been progressively reduced from 40 Mc/s to 5 Mc/s.

II. The Method of Position Measurement

The swept-frequency interferometer measures the east-west coordinate of the centroid of an isolated source situated on or near the solar disk. The measurement is made effectively simultaneously at six to eight different frequencies between 40 and 70 Mc/s. Such measurements can be made at successive times separated by $\frac{1}{2}$ s, but in the case of type II bursts the shortest time interval used has been 10 s. The aerials are fixed in orientation and normally position measurements are made only between 00 and 04 hr U.T. each day.

The principles of operation and technical details of the interferometer, and the method of analysis of records, have been fully described elsewhere (Wild and Sheridan 1958; Wild, Sheridan, and Neylan 1959). Briefly, the radio emissions received at two aerials, 1 km apart (long base line) on an east-west base line, are multiplied in a central receiver whose frequency is swept twice per second through the range 40–70 Mc/s. The swept-frequency modulation pattern is converted into a square waveform by passing through a high-gain amplifier, and displayed as intensity-modulated lines on paper records using a facsimile recorder. When sufficiently intense and persistent solar radiation is received the record appears banded. The position of the centroid of the source is found by measuring the positions of the edges of the "source" bands relative to a reference pattern which is superimposed on the record. This reference pattern corresponds to a source situated precisely at the centre of the Sun's disk. A second interferometer with shorter base line ($\frac{1}{4}$ km) is used for lobe identification.

III. The Observational Data

The times and positions of the type II bursts are listed in Table 1, together with spectral features of the bursts, positions of preceding type III bursts, and details of the

TABLE 1

POSITION AND SPECTRAL DATA FOR 22 TYPE II EVENTS

Date	Starting Time Type II Burst (U.T.)	Duration of Type II Emission (min)		M* or S	F† or H	Flare			Position Coordinates						Spectrum of Type II Burst	Remarks
									Flare	Type III Burst (50 Mc/s)	Type II Burst					
		Burst	Comp.			Heliographic Position		Imp.			45	50	55	60		
1958																
June 26	0304	15		S	U	10N	49E	2	+11·3	—	+36·6	+32·9	+29·6	+28·7	Multiple bands	Position measured on short base only
July 7	0033	10		S	U	25N	08W	3+	− 2·6	− 2·2	− 6·2	− 4·1	− 6·3	—	Two features, probably not harmonically related	Less likely flare identification is 25N, 07E, 1+
				S	U						− 2·0	− 0·2	− 0·5	+ 0·2		
	0101	7		M	U					−13·4	− 2·4	+ 0·6	+ 1·6	+ 2·7	Multiple bands and fine structure	Possible ionospheric scintillations
	0107	9		M	U						+ 0·6	+ 3·0	+ 3·0	—		

* M: position of source changes with time at a single frequency; S: no change of position at single frequency.

† F = fundamental band, H = second harmonic band, U = unidentified band.

TABLE 1 (*Continued*)

Date	Starting Time Type II Burst (U.T.)	Duration of Type II Emission (min)		M* or S	F† or H	Flare		Position Coordinates					Spectrum of Type II Burst	Remarks
								Flare	Type III Burst (50 Mc/s)	Type II Burst				
		Burst	Comp.			Heliographic Position	Imp.			45	50	55	60	
1958														
Aug. 20	0046	18		S	F	15–16N 16–18E	2–3	+ 4·2	+11·2	+24·4	+22·9	+21·3	+20·5	F very broad band	Preceded by continuum emission at +12′ to +15′.
				S	H					+10·2	+ 9·3	+ 8·7	+ 8·3		Possible slow movement of F band towards centre of disk
26	0021	18		S	U	20N 54W	3	−10·8	—	−27·8	−27·2	−24·8	−24·3	Broad band, complex	Fast ionospheric scintillations
1959															
Feb. 3	0054	12	8	S	H	12N 8E	2	+ 1·4	—	− 0·4	− 0·5	− 1·0	− 1·9	Possibly 2 bursts overlapping in time	
			3	S	H					+ 6·5	+ 7·3	+ 8·8	+ 7·6		
Feb. 9	0208	7		S	F	13N 90E	2	+14·2	+25·4	+19·6	+19·4	+20·6	+14·3	Fine structure	
	0231	14		M	H					+14·3	+14·8	+13·4	+11·9	F wispy	Movement at higher frequencies only

TABLE 1 (*Continued*)

Date	Starting Time Type II Burst (U.T.)	Duration of Type II Emission (min)		M* or S	F† or H	Flare		Position Coordinates						Spectrum of Type II Burst	Remarks
								Flare	Type III Burst (50 Mc/s)	Type II Burst					
		Burst	Comp.			Heliographic Position	Imp.			45	50	55	60		
1959															
July 10	0222	24	4	S	H	20N 63E	3	+13·5	+35·2	+32·6	+31·7	+31·7	+31·5	Short duration features	
			6	S	H					+29·2	+25·5	+24·9	+24·6	in irregular continuum	
14	0344	18		M	F	12–20N 0–10E	3+	+ 2·2	− 5·2	+14·5	+14·6	+13·1	—	Multiple bands	See Plate 1
	0358	12	9	?	F					−19·4	−18·0	−16·0	−13·0	Multiple bands	
				M	H					−23·8	−21·3	−21·0	−21·0		
			3	S	H					−14·9	−13·1	−11·9	−11·0	Merges into type IV continuum	
Aug. 17	0334	5		M	F	14–15N 15–16W	1	− 3·1	+ 3·2	—	—	− 0·9	− 1·7	Multiple bands, high frequency event	
Dec. 8	0121	5		S	F	10–12N 19–22W	2	− 8·3	−13·0	−20·2	−17·4	−16·5	−14·4	High frequency event. Multiple bands	
1960															
April 28	0122	24	18	S	F	55N 34E	3	+ 8·0	—	+23·9	+21·1	+19·1	+19·1	Broad band, split band,	See Plate 2
				S	H					+11·9	+ 9·2	+ 7·8	+ 7·3	herringbone	
			2	S	U					+32·8	+32·4	+26·1	+24·3	Separate bands overlapping	
			5	S	F					+19·1	+12·5	+ 9·2	+ 7·3	main burst, with different frequency drift rates	
			5	S	U					+ 0·3	− 3·7	− 5·0		Wispy, amorphous, no frequency drift	

TABLE 1 (*Continued*)

Date	Starting Time Type II Burst (U.T.)	Duration of Type II Emission (min)		M* or S	F† or H	Flare			Position Coordinates						Spectrum of Type II Burst	Remarks
									Flare	Type III Burst (50 Mc/s)	Type II Burst					
		Burst	Comp.			Heliographic Position		Imp.			45	50	55	60		
1960																
June 15	0300	17	17	S	H	22N	53W	1	−12·0	−15·2	−12·8	−13·5	−14·7	−16·6	Two single narrow bands with different frequency drift rates F amorphous	Note reverse sense of spread. Less likely flare identification 18N 13W. See Plate 3(*a*)
			2	S	H						—	—	−21·0	−19·5		
20	0131	10		S	H	13–17S	59–60W	2	−12·5	−31·0	−28·9	−26·5	−25·3	−24·7	F wispy Multiple bands	
27	0004	3	1	S	F	7– 9S	34–35E	2–3	+ 9·4	—	—	—	− 3·8	− 1·1	Single, narrow band. Herringbone	
			2	M	F						−17·2	−12·8	−11·0	—	Herringbone, no frequency drift	
29	0150	12		M	F	23N	56W	1	−12·5	—	−13·6	−16·4	−17·6	—	Wispy fine structure	
				M, S	H						−20·9	−18·1	−17·0	−16·0		Rapid outwards movement followed by stationary phase

TABLE 1 (*Continued*)

Date	Starting Time Type II Burst (U.T.)	Duration of Type II Emission (min)		M* or S	F† or H	Flare			Position Coordinates						Spectrum of Type II Burst	Remarks
									Flare	Type III Burst (50 Mc/s)	Type II Burst					
		Burst	Comp.			Heliographic Position		Imp.			45	50	55	60		
1960																
July 26	0334	3		S	F	9N	31W	1	− 7·5	—	−17·1	−15·3	−15·2	−15·0	Complex herringbone	
Sept. 2	0244	8		S	F	14S	54W	2	−13·2	−22·8	−25·2	−22·7	−20·7	−19·1	Wispy F	
Oct. 14	0156	4		S	F	8N	42W	1	− 9·6	—	—	−31·3	−29·3	−27·7	Split band	
Nov. 15	0221	18		M	U	26N	33W	3+	− 5·7	−11·2	—	+ 0·3	− 0·8	− 1·4	Complex broad band merging into type IV continuum	Movement slow
1961																
Jan. 3	0211	12		M	H	15S	36E	1	+ 9·1	—	+24·5	+20·6	+20·2	+18·3	Single band F amorphous	
April 6	0017	4		M	F	14N	1W	1	− 2·9	—	−14·5	−11·8	−10·7	− 9·3	Herringbone with very slow frequency drift	See Plate 3(*b*)
July 28	0233	18	4	M	F	12N	36W	2+	− 8·6	—	−24·5	−24·4	−24·3	−24·4	Complex broad band herringbone	Second part of burst (not listed) shows rapid inward movement followed by stationary phase (measurements only available on short base)

optical flares* with which the radio emissions have been associated. The tabulated positions are the angular displacements, in minutes of arc, of the sources (both optical and radio) from the centre of the Sun's disk, measured in the terrestrial east-west direction and in the case of the radio sources averaged over frequency bands 5 Mc/s in width.

Before proceeding to a detailed analysis of the position data, we describe the principles underlying the description and classification of the bursts and consider the relation between spectral features and the position of the source on the Sun's disk.

(*a*) *Spectral Features*

The brief descriptions of the spectra given in Table 1 are based on the notable features enumerated by Roberts (1959), namely, bandwidth (narrow unless noted to the contrary), harmonic structure, band splitting (secondary doubling into a pair of ridges), multiple bands (independent drifting bands neither harmonically related nor caused by band splitting), herring-bone structure, and other fine structure.

Since the relative positions, at a given frequency, of the fundamental and second harmonic bands of the same burst may be decisive as to a theory of the origin of the radio emissions, the harmonic bands with which the measured positions have been associated are listed separately. An identification has been made only if both bands are present in the spectrum; if they are not, or if the burst is too complex for satisfactory harmonic identification, the listing is "unidentified".

(*b*) *Multiplicity of Events*

Of the 22 events listed in Table 1, three are characterized by multiple bursts, separated in time, which are associated with the same flare. Separations in onset of the separate bursts of these events range from 14 to 34 min. In one case, the event of July 14, 1959 which is illustrated in Plate 1, the sources of the bursts are widely separated in position. For the other two events the positions of the individual bursts are closer but not coincident.

Seven other examples of multiple bursts are to be found in Table 1. These differ from the previous examples only in that the multiple nature of the burst was first recognized from the position data rather than from obvious temporal separation of the individual bursts. Once the multiple nature of the burst has been recognized, it has always proved possible to identify the components of the bursts with definite spectral features. The converse—that different spectral features imply different position coordinates—is certainly not true. Two further outstanding examples of multiple bursts are illustrated in Plates 2 and 3(*a*). The burst of April 28, 1960 is the most complex burst encountered during the investigation. The two bursts illustrated in Plates 2 and 3(*a*) are characterized by overlapping spectral bands with different

* For events preceding October 1960, the identifications given by Boorman *et al.* (1961) have been accepted. For subsequent events, flare data have been taken from reports issued by C.R.P.L. and the Fraunhofer Institute. A few cases of ambiguity have been resolved by appeal to 200 Mc/s position data. For two of the events, less probable but possible indentifications are also given in Table 1.

frequency drift rates, and in these cases there is little doubt that one is dealing with two disturbances moving independently through the corona at the same time but with different speeds. This is the optimum condition for recognition of multiple bursts. Overlapping spectral bands with different drift rates are rare, and in all the other cases of multiple bursts the components are recognized not simultaneously but in succession, and the drift rates of the bands associated with the components are comparable. The recognition of the multiple character of the bursts from spectral features alone is thus quite difficult and uncertain. The interferometer, of course, will yield only a mean position if two or more sources of comparable strength are active simultaneously, and multiple bursts may actually be more common than the 1 in 2 suggested by the cases listed.

The complexity of the type II burst may be matched by complexity in the associated flare, as for example in the events illustrated in Plates 2 and 3(*a*). This corresponding complexity of radio and optical events is of special interest to the theory of burst generation.

(*c*) *Band Splitting*

Many type II bursts show a secondary doubling of the bands. This phenomenon is known as band splitting. In these events both the fundamental and second harmonic bands are split into a pair of ridges (often similar in structure) whose separation in frequency is usually small compared with that between the two harmonic bands. Magnetic splitting, analogous to the Zeeman effect, has been suggested as the cause of band splitting (Wild, Murray, and Rowe 1954; Roberts 1959). Sturrock (1961) has advanced an alternative proposal that the two ridges of a split band are to be ascribed to preferential excitation, in a magnetic field, of two modes of propagation with zero group velocity.

None of the above examples of bursts with two or more components clearly differentiated in position can be associated with band splitting. The present sample of type II bursts contains only three possible, and poor, cases of band splitting. In none of these bursts is there any evidence for position changes exceeding 1′ at a given frequency over the duration of the burst. This suggests, but by no means establishes, that the sources of the two ridges of a split band are coincident in position and therefore in height in the solar atmosphere. Such a result is consistent with the above-noted suggestions that band splitting originates in a magnetic field at the seat of the radio emission.

(*d*) *Bursts with Apparent Movement*

One-third (13 out of 39) of all the bursts listed in Table 1 exhibit significant changes of source position with time at a fixed frequency. This behaviour is most plausibly interpreted as movements of the source tangential to the surfaces of constant plasma frequency. A full discussion of these bursts will be deferred until Section VI; we wish here only to illustrate the basis on which bursts have been classified as moving or stationary on the disk. The basic criterion is the presence or absence of temporal changes in position of the source *at a single frequency*. A burst is classified as moving on the disk only if the movement is pronounced, is similar at all frequencies, and

persists over the greater part or all of the duration of the burst. Where the movement is irregular in time or with frequency, or has a duration short compared with that of the burst, the burst has been classified as stationary on the disk. In such cases the changes in position are more likely to be due to irregular variations in the brightness distribution of the source at different frequencies, associated with an irregular shock front and irregularities in the electron density in the corona, or to irregular ionospheric refraction.

(e) *Position on the Disk and Spectral Features*

As may be seen from Figure 1, both type II bursts and the flares with which they are associated are approximately uniformly distributed in position coordinates* over the radio and optical disks. The distribution of flares is similar to those already obtained by Roberts (1959) and by Maxwell and Thompson (1962). The distribution

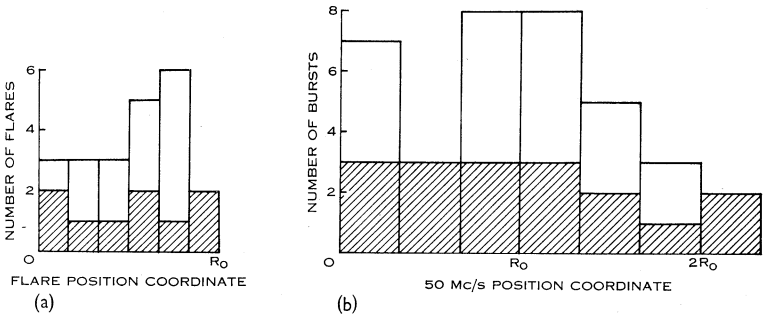

Fig. 1.—Distribution across the solar disk of 50 Mc/s position coordinates of the sources of type II bursts, and of the optical flares with which the bursts are associated. Events on the eastern half of the disk are shown cross-hatched, those on the western half in clear.

of type II bursts resembles closely that obtained by Wild, Sheridan, and Neylan (1959) for type III bursts (see also Fig. 9). The association of bursts with limb flares has been taken as an indication that the radiation is emitted in a very broad cone.

Roberts (1959), in his discussion of the earlier Dapto sample of type II bursts, pointed out that the intensities of the two harmonic bands were usually quite similar, but that there were a number of examples of bursts in which the second harmonic band was more intense than the fundamental. Perusal of the spectra of the bursts in the present sample reveals the interesting fact that the intensity of the second harmonic band, relative to the fundamental, tends to be much stronger for bursts associated with flares nearer the limb (heliographic longitudes $>45°$) than for those associated with more central flares. More decisive still, the definition of the fundamental band in limb events may become very poor, and the second harmonic band may be quite clearly defined whilst the fundamental band has a blobby or amorphous structure (Plate 3(*a*)), or takes on a wispy appearance resembling a series of narrow-

* The position coordinate is the projected distance between the centre of the disk and the source measured in the terrestrial east-west direction. It is usually given in units of the photospheric radius R_0, but occasionally, as in Table 1, in minutes of arc.

band, short-duration bursts following each other in rapid succession. These differences are most pronounced at low frequencies and do not always show up when the frequency of the fundamental band exceeds 50 Mc/s. They are a confirmation of a suggestion by Wild, Sheridan, and Neylan (1959) that an apparent absence of harmonic pairs in type III bursts beyond the normal radio limb could be due to the absence of the fundamental band.

These spectral features suggest that the escape of the second harmonic emission is virtually unimpeded in all directions within a cone whose semi-angle approaches $\frac{1}{2}\pi$, whereas for events near the radio limb emission at the fundamental frequency suffers heavy attenuation and irregular scattering during its outward passage. This explanation is consistent with the proposal advanced by Roberts that the escape of the fundamental band in limb events is made possible by wide-angle scattering on small-scale irregularities in the corona near the plasma level for the radiation in question. The existence of irregularities whose scale is small compared with the size of the source is also an integral part of the plasma hypothesis, since it is held responsible for the escape of the fundamental emission over a fairly wide cone. If, as seems probable, type II and type III bursts are generated in dense, radial coronal streamers, the poor definition in the fundamental band for limb events suggests that the irregularities scatter the radiation less efficiently and reliably at wide angles to the axial direction of the coronal streamer.

IV. Confirmation of the Plasma Hypothesis

In the idealized case,* when refraction is negligible and ejection is radial and different frequencies are assumed to originate at different fixed levels in the solar corona, the plasma hypothesis predicts that:

(i) at a fixed frequency, the burst position is a linear function of the flare position;

(ii) for a single burst, there is a systematic variation of position with frequency, with the distance from the centre of the disk increasing with decreasing frequency. The variation $P_1 - P_2$ between the positions for any two frequencies is a linear function of burst position P_2.

To explore the validity of the plasma hypothesis, we now take the data listed in Table 1 for type II bursts. These data are plotted in Figures 2(*a*) and 3(*a*). Figure 2(*a*) illustrates the relation between 50 Mc/s burst position and flare position, and Figure 3(*a*) compares the difference in position $P_{45} - P_{60}$ with the 60 Mc/s position coordinate. Each symbol in these diagrams represents the mean value for a single burst. In general the variation of position with frequency for a given burst does not change with time; in those rare cases where it does, a mean value has been plotted in Figure 3(*a*).

The plasma hypothesis is also relevant to type III bursts, and a comparison between type II and type III bursts is of interest. We have therefore plotted in Figure 2(*b*) the relation between 50 Mc/s burst position and flare position for the type III bursts listed in Table 1, and in Figure 3(*b*) the relation between $P_{45} - P_{60}$ and P_{60} for the sample of type III bursts studied by Wild, Sheridan, and Neylan (1959).

* The model is illustrated in Figure 7, Appendix I, with $\beta = 0$.

On the average, the data presented in these four diagrams appear to conform to the predictions of the plasma hypothesis. Amongst the individual points, however, there is a large scatter, whose origin should be examined before a decisive test of the plasma hypothesis is attempted. This scatter is not due to inaccuracies of measurement of the plotted mean positions, as we now show. In Table 2 are summarized some

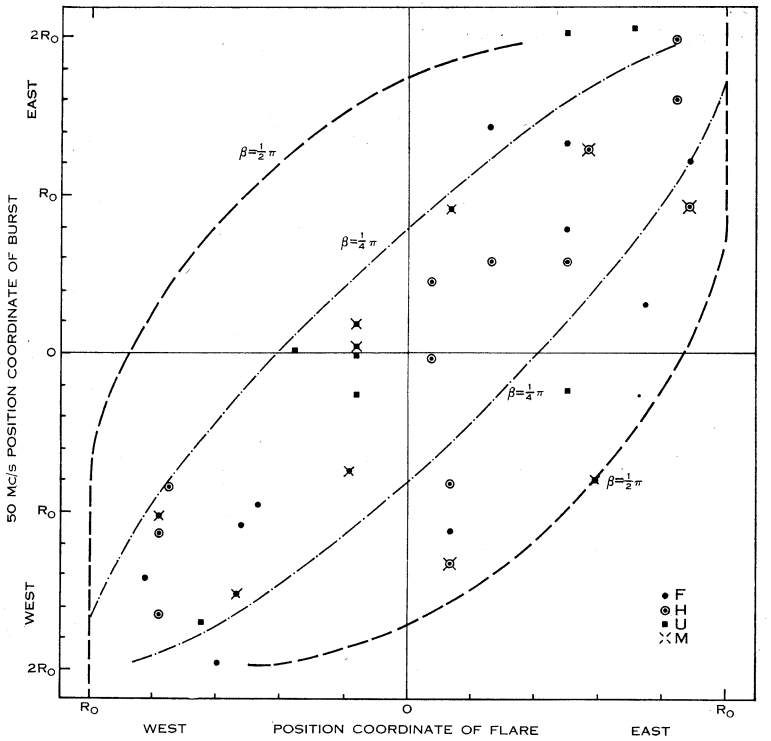

Fig. 2(a).—Observed position coordinates of the sources of type II bursts at 50 Mc/s, plotted against the position coordinates of the associated optical flares. If more than one burst is associated with the same flare, points for each burst are shown. Fundamental bands (F), second harmonic bands (H), and unidentified bands (U) are distinguished. Positions of the bursts designated "M" change with time at a single frequency. β is the angular dispersion of the directions of the disturbances from the radial direction (see Appendix I). The pairs of dashed curves for given β define envelopes in the position coordinate system for non-radial ejection of the exciting disturbance from the region of the flare. They are drawn for $R_{50}/R_0 = 2{\cdot}0$.

estimates of the accuracy of a single measurement of position within a 5 Mc/s frequency band. Causes of inaccuracy include both reading errors and inaccuracies due to poor definition of the edges of the "source" bands on the interferometer records.* These estimates indicate that the probable error in a single position measurement is approximately $\pm 2'$. Most of the mean positions for type II bursts are based on an average

* Causes of poor definition of the edges of the "source" bands are low source intensity and irregular fluctuations of both ionospheric and solar origin.

of 10 or more individual measurements. Hence the error of measurement in a mean position plotted in Figure 2(*a*) is approximately $2/\sqrt{10} = 0{\cdot}6'$. The error in the points in Figure 3(*a*) is $\sqrt{2}$ times larger, or $0{\cdot}9'$ approximately. These probable errors are far less than the scatter in the respective diagrams.

The scatter could be due to several causes. These are

(*a*) irregularities in the electron density distribution in the corona;

(*b*) non-radial ejection of the exciting disturbance;

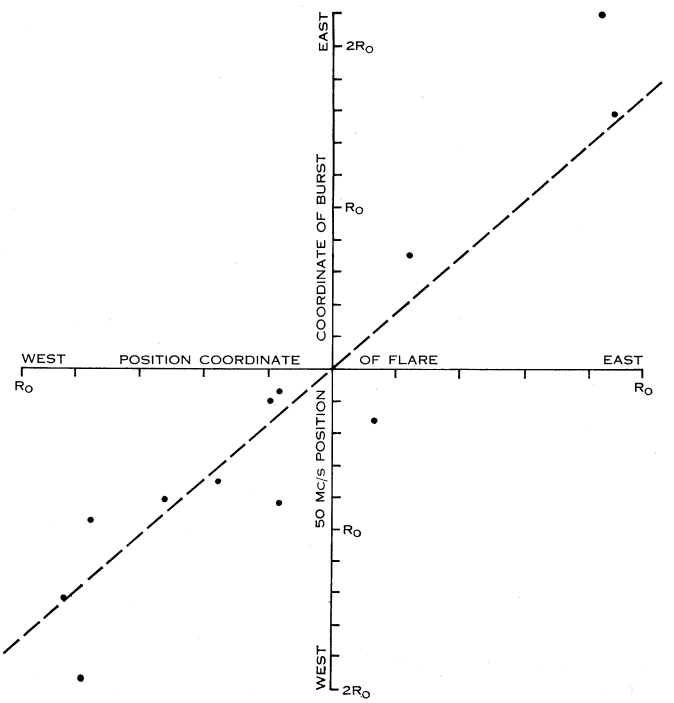

Fig. 2(*b*).—Observed position coordinates of the sources of type III bursts at 50 Mc/s, plotted against the position coordinates of the associated flares. These bursts, whose harmonic structure is not known, preceded the type II bursts of Figure 2(*a*). The dashed line is the least squares fit to all the points in Figure 2(*a*).

(*c*) irregular ionospheric refraction.

These disturbing influences will now be examined in turn.*

* Irregular refractions in the solar atmosphere may be an additional cause of scatter. Wild, Sheridan, and Neylan (1959) and Shain and Higgins (1959) have examined the extent to which the apparent position of a source located at the plasma level in the irregular but quasi-spherical corona may be affected by refraction in the solar atmosphere. They concluded that the measured positions could be interpreted as giving directly though approximately the true projected positions of the sources. Their interpretation has been adopted here.

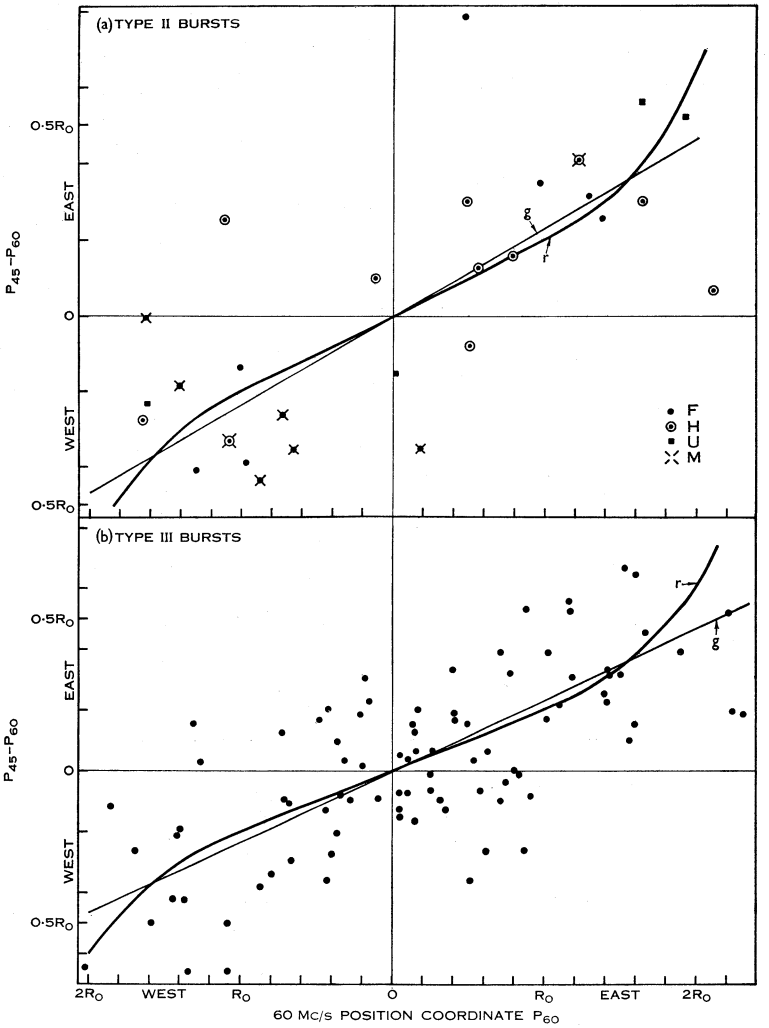

Fig. 3.—Diagrams showing the dependence of variation of position with frequency, $P_{45}-P_{60}$, on the 60 Mc/s position coordinate P_{60}. Each symbol represents the mean value observed for an individual burst. (*a*) *Type II bursts.* The symbols F, H, U refer to the harmonic structure of the bursts (F = fundamental, H = harmonic, U = unidentified), and M denotes bursts with movement on the disk. (*b*) *Type III bursts* (from Wild, Sheridan, and Neylan 1959). The harmonic structure of these bursts is not known. Note that the scale of the ordinate for type III bursts is 0·8 times that for type II bursts.

If it were assumed that the true sources are located at constant heights, h_{60} and h_{45}, in the solar atmosphere and that propagation is linear, then the slope of the best-fit *straight line* through the points would give the value of $s = (h_{45}-h_{60})/h_{60}$. If, on the other hand, ionospheric wedge refraction is present, the line on the graph corresponding to given s becomes curved or modified in gradient. The curves shown by the full lines correspond to $s = 0{\cdot}2$, assuming (i) that the degree of ionospheric scatter is given by the observed scatter of the points in this diagram, and (ii) that the true east-west distribution of sources on the disk is either Gaussian (curve *g*) or rectangular (curve *r*). See Appendix II.

(*a*) *Variations in the Height of the Plasma Levels in the Corona*

Irregularities in the corona will produce variations in the heights of emission levels from event to event. The scatter in burst positions at a single frequency, due to this cause, should vanish at the centre of the disk and increase steadily towards the radio limb. This behaviour is not observed (Fig. 2(*a*)), and we conclude that coronal variations are not the dominant cause of the scatter in the mean burst positions. Moreover, random variations in the electron density will not introduce any systematic variation of position with frequency.

(*b*) *Departures from Radial Motion*

Using a simple model, the scatter in the positions of bursts generated by non-radial exciting disturbances is evaluated in Appendix I. The envelopes sketched in

TABLE 2

SUMMARY OF TESTS OF SIGNIFICANCE OF THE VARIATION OF POSITION WITH FREQUENCY FOR TYPE II BURSTS

Date	Effective Number of Measurements	R.M.S. Deviation of an Individual Measurement (min of arc)
20.vii.58	11	1·63
8.xii.59	11	2·05
28.iv.60	22	2·55
15.vi.60	10	1·63
20.vi.60	18	1·26
27.vii.60	8	2·12
6.iv.61	23	1·43

Figure 2(*a*) define the limits within which all the observed points should lie for the chosen values of β, where β is the semi-angle of the possible cone of ejection of the disturbance about the radial direction. When it is considered that other phenomena are undoubtedly contributing to the scatter, it seems reasonable to infer that for the majority of type II bursts β is certainly less than $\frac{1}{4}\pi$ and hence that in general the motion of the disturbance is not markedly non-radial. As a class, the disturbances exciting type III bursts appear to depart from radial motion to a much lesser extent than the exciters of type II bursts (see Fig. 2(*b*)). In Appendix I it is also shown that the scatter in the difference in position $P_{45}-P_{60}$ decreases from 2′ for $\beta = \frac{1}{4}\pi$ (3′ for $\beta=\frac{1}{3}\pi$) for bursts near the centre of the disk, to the very small values near the radio limb.

In testing the validity of the plasma hypothesis, non-radial ejection of the exciting disturbance may be disregarded unless the *average* direction of motion is

significantly non-radial, or unless $\beta \sim \frac{1}{2}\pi$ for the great majority of bursts. The former eventuality seems improbable, and the latter is contradicted by the observations.

(c) *Irregular Ionospheric Refraction*

The most troublesome complication in a test of the plasma hypothesis at our frequencies is undoubtedly irregular ionospheric refraction, which can generate a systematic variation of position with frequency (in the same sense as that predicted by the plasma hypothesis) as well as scatter in the measured positions. This systematic component of ionospheric refraction effects arises from a combination of two circumstances:

(i) displacement of source position by refraction is frequency sensitive (approximately as $1/f^2$);

(ii) if a source is *observed* close to or beyond the radio limb, it is much more likely to have been refracted in the direction *away from* than towards the centre of the disk.

Appendix II contains a mathematical formulation of these effects.

Since the effects of irregular ionospheric refraction cannot be isolated from the other causes of scatter, only an upper limit to the magnitude of the systematic component can be obtained. This upper limit has been evaluated (in Appendix II) by making the extreme assumption that the whole of the scatter in the points of Figures 3(*a*) and 3(*b*) is attributable to ionospheric refraction. It is shown in Appendix II that at our frequencies the systematic variation of position with frequency, predicted by the plasma hypothesis, will be increased by irregular ionospheric refraction by an amount which may be as large as 20%.

The full lines drawn in Figures 3(*a*) and 3(*b*) illustrate two predicted relations between $P_{45}-P_{60}$ and P_{60}, which have been fitted to the plotted points. The two curves relate to different distributions of the burst positions over the solar disk. The relations, which are derived in Appendix II, are obtained by combining the systematic variation of position with frequency generated by irregular ionospheric refraction with that predicted by the plasma hypothesis with $(P_{45}-P_{60})/P_{60} = 0{\cdot}2$. As mentioned above, in this particular instance ionospheric refraction contributes the permissible maximum of about 20% of the variation.

Despite their systematic nature, the effects of ionospheric refraction on the systematic variation of position with frequency should be dominated by the much larger plasma effects which we wish to examine. Nevertheless, the refraction effects may not be ignored in quantitative applications of the position data to studies of the structure of the solar corona.

Confirmation of the Plasma Hypothesis

We are now able to apply the data plotted in Figures 2 and 3 to a quantitative test of the validity of the plasma hypothesis. For this purpose the data have been analysed by the method of least squares. The positions of the flares and of the 60 Mc/s position coordinates have been assumed exact. The results are collected in Table 3.

Figure 2(*a*) indicates that at a given frequency the burst position coordinate increases with the flare position coordinate. The scatter in the points is so large that it is not possible to decide whether these two quantities are linearly related, as predicted by the plasma hypothesis, but if they *are* linearly related, the slope for type II positions at 50 Mc/s is $1{\cdot}73 \pm 0{\cdot}22$. The slope of the relation is thus almost 8 times as large as its standard deviation.

For both type II and type III bursts the systematic variation of position with frequency increases from centre to radio limb (Figs. 3(*a*) and 3(*b*)). The ratio of $P_{45}-P_{60}$ to P_{60} is $0{\cdot}20 \pm 0{\cdot}039$ for type II bursts, and $0{\cdot}20 \pm 0{\cdot}023$ for type III bursts. The

TABLE 3

RESULTS OF REGRESSION ANALYSIS FOR TYPE II AND TYPE III BURSTS

Type of Burst	Harmonic* Structure	Number in Sample n	Regression Coefficient b	Standard Deviation from Regression s (in units of R_0)	Standard Deviation of Regression Coefficient s_b	$s_b\sqrt{n}$
(*a*) Regression of P_{50} on P_{flare}						
II	F	11†	1·97	0·53	0·28	0·93
	H	11†	1·66	0·38	0·18	0·60
	U	9†	2·07	0·73	0·55	1·65
	All	36	1·73	0·71	0·22	1·32
(*b*) Regression of $P_{45}-P_{60}$ on P_{60}						
II	F	9	0·26	0·28	0·091	0·27
	H	11	0·12	0·19	0·054	0·18
	U	8	0·25	0·21	0·064	0·18
	All	28	0·20	0·23	0·039	0·21
III	—	89	0·20	0·22	0·023	0·22

* See Table 1 for definition of symbols.

† Bursts with markedly non-radial motion excluded.

values of these ratios, and hence their statistical significance, will be decreased when irregular ionospheric absorption is taken into account, but after this is done the probability that the observed systematic variation of position with frequency could arise by chance remains very small.

The second of these statistical tests relates to the differentials of positions observed near the two extremes of our operating range of frequencies. Its positive result is greatly increased in significance by the pronounced ranking of positions by frequencies which is exhibited at *all* frequencies by bursts sufficiently far removed from the centre of the disk. This ranking is illustrated in Figure 4 for all type II bursts (19 in all) with $|P_{45}| > 15'$. Of these 19 bursts, all except the two nearest the centre of the disk exhibit a systematic ranking of position with frequency, with

positions for the lower frequencies farther removed from the centre of the disk, as predicted by the plasma hypothesis.

These tests indicate that different frequencies originate at systematically different levels in the corona, and so provide confirmation of the plasma hypothesis.

V. Some Implications of the Position Data

We now explore some particular points which have emerged from the analysis of the position data.

(*a*) *Comparison of Positions of Bursts of Types II and III*

There is remarkable agreement between the statistical parameters which describe the average behaviour of the positions of the sources of type II and type III bursts.

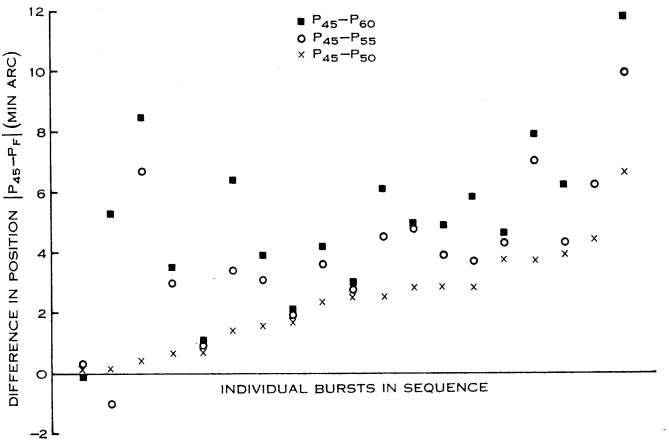

Fig. 4.—Position differentials, $|P_{45}-P_F|$, for non-central type II bursts ($|P_{45}|>15'$). Each group of three points refers to an individual burst. Bursts are arranged in order of increasing $|P_{45}-P_{50}|$.

As can be seen from Table 3, the agreement is most noticeable amongst the variation of position with frequency, whose regression on burst position and scatter (after correction for sample size) are identical for the two types of burst. The linear relation which we have deduced between type II burst position, P_{50}, and flare position, P_{flare}, fits type III bursts equally well—see Figure 2(*b*). These points of agreement are strong evidence that the radio emissions of type II and type III sources of identical frequency are generated in equivalent, though not necessarily identical, regions in the corona.

The agreement does not extend to the positions of individually associated type II and type III bursts. About half of the type II bursts in Table 1 are preceded by type III bursts whose positions rarely agree closely with the type II positions and frequently differ from them by more than 10′. Further, Figure 2 suggests that type III bursts show much less scatter in position than do the type II bursts with which they are associated. It has been proposed (e.g. Wild 1962) that both phases of a compound

type III-type II burst are generated by the same explosion within a flare. The points of disagreement would then imply that the exciting agencies for the two types of burst do not, in general, follow identical trajectories through the solar atmosphere.

One further implication of the general similarity in position of these two types of burst should be mentioned. The exciting disturbances generating type III bursts are believed to be fast streams of electrons, with velocities of the order of half the velocity of light (Wild, Sheridan, and Neylan 1959). It seems reasonable to assume that at such high velocities the exciting disturbance is unable to modify appreciably the electron density of the corona during its passage, and hence that the heights of emission levels measured for type III bursts will refer to the unexcited corona. It might be expected, however, that the far more slowly moving shock fronts exciting type II bursts may well modify the coronal electron densities at the seat of emission. Should they do so, the emission levels observed for type II sources would not refer to the unexcited corona, and would differ from the emission levels for type III bursts at identical frequencies. The similarity of the average emission levels for type II and type III bursts thus establishes the important result that the shock waves exciting type II bursts are unable to modify the electron densities in the corona to an extent which can be detected statistically.

(*b*) *Anomalous Positions of Sources of Harmonic Bands*

There are no statistically significant differences between the *general distributions* of the positions of the sources of fundamental and of second harmonic bands either as regards dependence on flare position or as a function of frequency. It should be mentioned, however, that the variation of position with frequency for second harmonic bands is *less* than for fundamental bands, and that the positions for second harmonic bands tend to lie *inside* the positions for fundamental bands. These results are consistent with the conclusion of Smerd, Wild, and Sheridan (1962) that in those few cases where a definite decision could be made, the position for the second harmonic band of a type II burst invariably lay *inside* the position for the fundamental band of the same burst.

At first sight this result seems inconsistent with the plasma hypothesis. An explanation in terms of preponderantly backwards radiation at the second harmonic frequency, followed by reflection at the plasma level appropriate to the harmonic frequency, has been proposed by Smerd, Wild, and Sheridan.

(*c*) *The Radial Distribution of Electron Density in the Corona*

Heights of the mean plasma levels in the frequency range 45–60 Mc/s can be estimated, although with uncertainty, from the position data enumerated in Table 1. Mean plasma levels so derived will refer to coronal densities relevant to the generation of type II and type III bursts, possibly within coronal streamers.

The height of the 50 Mc/s plasma level is given directly by the coefficient of regression of P_{50} (for fundamental bands) on P_{flare}. Thus, from Table 3, $R_{50}/R_0 = 1{\cdot}97$. Probably the most reliable estimates of the heights of the plasma levels for other frequencies are obtained from the mean ratios of the position coordinates for the

fundamental bands of stationary bursts for which $|P_{45}| \geqslant 15'$. These ratios are $R_{50}/R_{45} = 0{\cdot}91$, $R_{55}/R_{45} = 0{\cdot}87$, $R_{60}/R_{45} = 0{\cdot}80$. The resulting heights are plotted in Figure 5. It should be emphasized that these values have been obtained from a small sample of fundamental bands of type II bursts. They are, however, very similar to the heights found by Wild, Sheridan, and Neylan (1959) from a larger sample of type III bursts; their points for type III bursts are given in Figure 5.

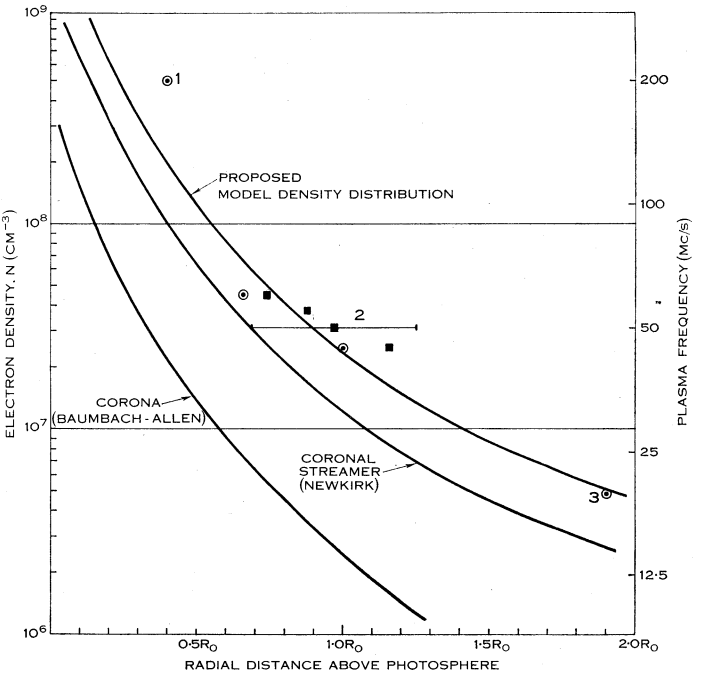

Fig. 5.—Average electron densities in the corona as a function of height. The full curves represent respectively the standard Baumbach-Allen corona, the density of the average coronal streamer as given by Newkirk (1961), and a streamer with twice the density given by Newkirk. The plotted points give the measured heights of origin of type II and type III bursts. ◉, type III bursts (Morimoto 1961; Shain and Higgins 1959; Wild, Sheridan and Neylan 1959). ■, type II bursts of the present analysis; the bar represents the probable error of the 50 Mc/s point and is typical of the errors in all four points for type II bursts.

Also plotted in Figure 5 are two other points, one for the 200 Mc/s plasma level (Morimoto 1961) and the other for the 19·7 Mc/s level (Shain and Higgins 1959). Both these points were obtained from type III bursts by methods rather similar to that adopted in this paper. Shain and Higgins have corrected their observations for the diurnal component of ionospheric refraction, but errors due to irregular refraction may remain. They also incline to the view that their measurements referred to fundamental bands. The harmonic structure of the 200 Mc/s bursts was not stated, and second harmonic bands may be included. Let us assume, by analogy with our result for the lower frequencies, that the sources of fundamental and second harmonic

bands at 200 Mc/s also agree closely in position. We may then use the results of these three independent investigations to study the distribution of coronal electron density over a wide range of heights.

From K-coronameter observations, Newkirk (1961) derived for the radial electron density distribution above the average active region the modified van de Hulst relation

$$N = 8{\cdot}3\times10^4\times10^{4{\cdot}32/R}\ \mathrm{cm}^{-3}.$$

This model distribution, and one with density twice as great, are reproduced in Figure 5. The latter, denser, model gives a good representation of the radio observations, although it predicts a variation $P_{45}-P_{60}$ whose value is little larger than half the observed value. As pointed out in Section IV, portion of the excess of the observed over the predicted systematic variation may be due to ionospheric refraction. In endeavouring to account for the remaining (perhaps major) part of the failure of the model to represent the observations near 50 Mc/s, we must seriously question the correctness of the model at heights exceeding 1 solar radius above the photosphere. The optical observations of Newkirk do not extend beyond this height, and at greater heights the model electron density distribution is fixed essentially by the single point at 19·7 Mc/s. Acceptance of the electron density gradient determined from our observations at 45–60 Mc/s implies that the height determined by Shain and Higgins at 19·7 Mc/s is too low, perhaps by as much as $0{\cdot}5R_0$. The possibility of an error as large as this cannot be dismissed. It is only twice as large as the error in the height deduced from the present analysis for the 50 Mc/s plasma level, and in our case the experimental conditions are much more favourable than at 20 Mc/s. The optical identifications for the type II bursts are almost invariably certain and are not accompanied by the difficulties and uncertainties involved in the identification of the flares and optical centres responsible for the type III bursts studied by Shain and Higgins. Also, at the lower frequency the effects of ionospheric refraction are much more troublesome.

In conclusion, we may say that at heights below 1 solar radius above the photosphere, the *average* coronal densities in the regions of generation of type II and type III bursts appear to exceed by a factor of about 2 the average electron densities determined optically for coronal streamers. The course of the electron density distribution at greater heights cannot be defined with any certainty from the available radio data.

VI. Tangential Movements and the Trajectories of the Exciting Disturbances

Included in Table 1 are 13 bursts, one-third of those listed, which exhibit systematic changes of position coordinates with time at a single frequency. Since displacement of a source from its true position, accompanied by movement, is characteristic of ionospheric scintillations, these bursts with movement on the disk demand careful scrutiny before the movements can be accepted as real.

Many of the moving bursts show no change with time in the systematic variation of position with frequency, as would be expected of sources whose positions are displaced by ionospheric refraction. This lack of variation is illustrated by the separate

bursts in the event of July 14, 1959 (Plate 1) and, still better, by the burst of April 6, 1961, for which the measured positions are reproduced in Plate 3(*b*). The rates of change of position with time confirm the constancy of the variation for this latter burst: for the 45, 50, 55, and 60 Mc/s bands the rates are respectively 2·9, 3·2, 2·5, and 2·8′/min. We conclude that for at least some of the moving bursts the changes in position coordinates cannot be eliminated by correction for supposed ionospheric refraction, and we shall tentatively accept the reality of, and a solar origin for, the changes in position.

The event of July 14, 1959 is compelling evidence that, in this instance at least, the source movements on the disk are due to a tangential component in the motion of the exciting disturbance in the solar corona. The displacements in position coordinates of the two separate bursts of this event, if extrapolated backwards in time, intersect near the projected position of the flare and near the time of the type III burst that presumably was generated by the same initial explosion in the flare. In view of the uncertainties in the interpretation of the data for bursts with movement on the disk, and the lack of direct measurements of the heights of the sources, no quantitative discussion will be attempted. It is, however, pertinent to add that the spectra of moving bursts as a class are characterized by little or no drift of frequency with time and by broad bandwidth, both of which are features to be expected in a radio burst generated by a shock front which is inclined at a large angle to the surfaces of constant electron density.

The rates of change of position with time, for those sources of fundamental bands which exhibit definite and regular movement on the disk, range from 1·1 to 2·9′/min, with a mean of 2·0′/min. To the extent to which the movements can be regarded as real, they imply tangential speeds of the order of 1000–2000 km/s. These speeds are similar to the radial speeds inferred from the rates of frequency drift of bursts stationary on the disk, which presumably are produced in equivalent regions of the corona.

It is not uncommon for the mean position of a moving burst to lie approximately radially above the position of the associated flare. If our hypothesis of tangentially moving sources is well founded, the trajectories of the shock fronts must sometimes be curved as well as non-radial. It may be surmised that a shock front following such a curved trajectory might eventually acquire a downwards component of velocity. One crucial test for the existence of movement with an inwards component would be the recognition of type II bursts with a drift of spectral features from low to high frequencies. Such bursts are very rare. Of over 130 type II bursts recorded with the Dapto spectograph since September 1952, only two can, with certainty, be placed in this category. One is the burst of April 5, 1957, described by Roberts (1959), and the other is the moving burst of June 27, 1960 (Table 1). In both cases a short period of positive frequency drift occurred at the end of the burst, after initial drift in the normal negative sense.

VII. Comparison with 200 Mc/s Positions

The 45–60 Mc/s positions of five type II bursts are compared in Figure 6 with the 200 Mc/s positions measured for the same bursts at the Tokyo Astronomical

Observatory. The smallness of the number of possible comparisons is due entirely to the comparatively low starting frequencies, less than 100 Mc/s, of the great majority of type II bursts. Indeed, in most cases of simultaneous activity in both frequency ranges, the high frequency activity is not at all directly related to the type II emission at the lower frequencies.

One feature, which has already been noted by Morimoto (1962), calls for comment. In three of the five events in Figure 6 the 200 Mc/s positions change with time. The rates of change of position are quite typical of the moving bursts already

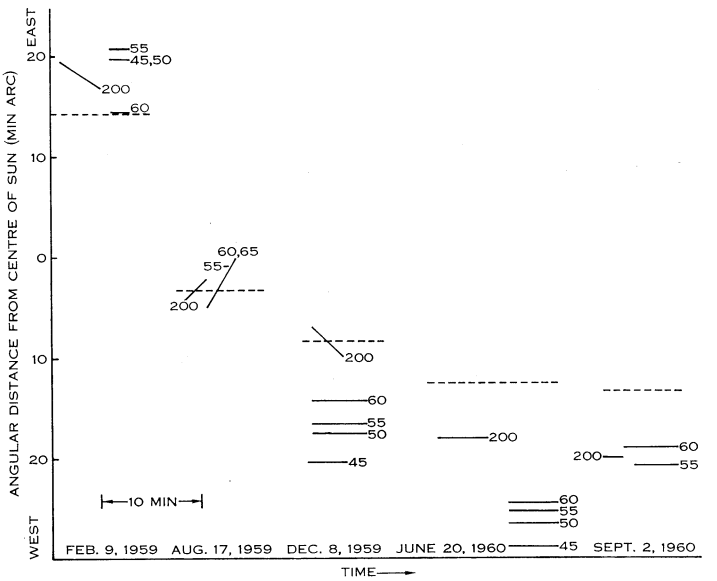

Fig. 6.—Comparisons of the positions of sources of type II bursts at 200 Mc/s and at 45–60 Mc/s. In each case the 200 Mc/s measurement refers to the second harmonic band and the lower frequency measurements to the fundamental band of the same burst. Flare positions are indicated by dashed lines. The 200 Mc/s measurements were made at the Tokyo Astronomical Observatory.

encountered at lower frequencies. It is rather disconcerting to find moving bursts at 200 Mc/s whilst the same bursts are stationary at the lower frequencies. On the other hand, the observations of moving bursts at high frequencies strengthens the arguments advanced in Section VI for the reality of the movements, since the movements at 200 Mc/s cannot be attributed to ionospheric refraction.

VIII. Discussion

This investigation has touched upon many aspects of the type II radio burst. These will now be enumerated and briefly discussed.

(i) *Confirmation of the Plasma Hypothesis.*—A detailed statistical analysis has shown that there exists a systematic variation of burst position with frequency.

The variation is statistically significant, and except near the radio limb is far greater than the variation to be expected from irregular ionospheric refraction. This result is a confirmation of the plasma hypothesis, in which it is supposed that the radio emission is generated by plasma oscillations excited in the coronal gas by a disturbance which moves outwards through the solar atmosphere. A more striking confirmation of the plasma hypothesis is the agreement between position data for type II and type III bursts, which will now be discussed.

(ii) *Similarity in Positions of Type II and Type III Bursts.*—There is quite remarkable similarity, on the average, between the statistical parameters which describe the behaviour of the positions of type II and type III bursts. Almost identical results are obtained for the two types of burst in respect of the relations between flare position and burst position, and between variation of position with frequency and burst position. This agreement suggests very strongly that the sources of the emission of these two distinctive types of burst are located in equivalent regions in the corona. It is thought that the exciters of these two types of burst differ widely in physical nature and in speed of motion through the corona—magnetohydrodynamic shock fronts with speeds $\sim c/300$ for type II bursts, streams of electrons with speeds $\sim c/3$ for type III bursts. The common features of the two types of burst are thus attributed to the properties of the plasma oscillations generated by the two types of exciting disturbances, rather than to the exciters themselves. An additional implication of this similarity in position for the two types of burst is that the shock fronts exciting type II bursts appear not to modify the electron density distribution in the corona to an extent which can be detected statistically.

(iii) *Multiplicity of Bursts.*—The position measurements have demonstrated that multiple type II bursts are much more common than had been inferred previously from spectral data alone. Many events consist of two or more bursts, either simultaneous in time or following in quick succession, whose source positions and rates of frequency drift may differ widely. Presumably these multiple bursts are excited by multiple shock fronts, ejected in quick succession from the vicinity of the flare, which follow different trajectories with different speeds through the solar atmosphere. The complexity of the radio event is matched by complexity in the associated flare. A satisfactory theory of the initiating explosion responsible for the type II event, which is as yet in a very rudimentary form, must include the possibility, as a normal aspect of the process, of the ejection of multiple shocks in different directions.

(iv) *Tangential Movements of the Sources.*—An analysis of the position of the burst in relation to the position of the associated flare leads to the conclusion, already suggested by the different positions of the sources of multiple bursts, that the trajectories of the exciting shock fronts are often non-radial. For the majority of bursts the departures from radial motion are not large ($<45°$), but in a few cases the ejection appears to be almost tangential to the Sun's surface. Tangential motions of exciting disturbances have also been inferred from the systematic changes of position with time of a source at a single frequency, which occur in about a third of the events studied. One pitfall of which we are fully aware is that such temporal changes in position could be caused by ionospheric scintillations. However, the evidence

indicates that the position changes are of solar origin and do in fact indicate tangential movement of the source. This view is supported by the observation that the spectra of moving bursts as a class are characterized by little or no drift of frequency with time and by broad bandwidth, both of which are features to be expected in a radio burst generated by a tangentially moving source.

Some care, however, is needed when speaking of tangential movements. A single *position* measurement gives the position coordinate of the source projected onto the solar disk. This position, considered in relation to the flare position, indicates, though with some uncertainty, whether the source of the burst lies radially above the flare. However, a temporal change in position of the source at a single frequency indicates only that the source possesses a component of motion *parallel to the surfaces of constant plasma frequency*. In the disturbed corona there is no reason to expect that surfaces of constant plasma frequency should be parallel to the solar surface. It is perhaps not too much to hope that simultaneous measurements of position and rate of change of position of a source at a single frequency, and of the rate of frequency drift from the spectrum, could result in systematic mapping of the electron density contours in the vicinity of a source. Such a program, of course, calls for position measurements in two dimensions and cannot be attempted with the restricted position measurements currently available. It remains as an intriguing problem for the future.

(v) *Position on the Disk and Spectral Features.*—For bursts near the radio limb there is a tendency for the intensity of emission in the fundamental band to be much weaker than the emission in the second harmonic band and for the definition of the fundamental band to be poor. These effects are attributed to scattering and attenuation of the emission in the fundamental band.

(vi) *Relative Positions of the Sources of Fundamental and Second Harmonic Bands.*—There are no statistically significant differences between the positions, measured at identical frequencies, of the sources of the two bands. This curious result appears to be inconsistent with the plasma hypothesis. An explanation involving propagation effects has been proposed by Smerd, Wild, and Sheridan (1962).

(vii) *Split Bands.*—The limited data available suggest that the sources of the emission in the two ridges of the split band are identical. This is consistent with a magnetic origin for the splitting, but further observations are needed to place the issue beyond doubt.

(viii) *The Electron Density Distribution in the Corona.*—Analysis of the position data leads, with some uncertainty, to an average radial distribution of electron density over the limited region of heights accessible to the interferometer. This distribution has been extended to both greater and smaller heights by appeal to the positions of type III bursts measured at other frequencies. The result does not differ greatly from the electron density distribution found optically for the average coronal streamer.

One final feature which should be mentioned is the formal statistical approach adopted for the analysis of the position measurements. This approach offers several advantages. In dealing with such a comparatively rare and complex phenomenon

as the type II burst, this treatment minimizes the possibility of drawing unwarranted conclusions from scanty data. Of more importance, the statistical treatment permits a realistic estimate of the errors of measurement. Such an estimate must precede a proper assessment of the physical importance of the scatter in the measured positions, which in turn determines the accuracy with which such physical properties as the mean heights of the levels of given plasma frequencies in the solar corona can be derived. In fact, the question of the estimation of observational errors is basic to almost any observational approach to the quantitative determination of the structure of the solar atmosphere.

IX. Acknowledgments

The author is greatly indebted to Mr. J. P. Wild for much helpful discussion, advice, and encouragement. This study would not have been possible without the series of records obtained over the last few years with the Dapto radio spectrograph and the swept-frequency interferometer. For these excellent records acknowledgment is made to K. V. Sheridan, G. H. Trent, and J. Joisce, and also to the many people who have contributed to their processing and analysis. Mr. K. V. Sheridan was also particularly helpful in the interpretation of the records. The author wishes to thank Dr. M. Morimoto of the Tokyo Astronomical Observatory for the provision of much data on 200 Mc/s bursts, and Professor W. R. Steiger of the University of Hawaii for optical photographs of the flare of April 28, 1960.

X. References

Boorman, J. A., McLean, D. J., Sheridan, K. V., and Wild, J. P. (1961).—*Mon. Not. R. Astr. Soc.* **123**: 87.

Maxwell, A., and Thompson, A. R. (1962).—*Astrophys. J.* **135**: 138.

Morimoto, M. (1961).—*Publ. Astr. Soc. Japan* **13**: 285.

Morimoto, M. (1962).—*J. Phys. Soc. Japan* **17** (Suppl. A–II): 220.

Newkirk, G. (1961).—*Astrophys. J.* **133**: 983.

Roberts, J. A. (1959).—*Aust. J. Phys.* **12**: 327.

Shain, C. A., and Higgins, C. S. (1959).—*Aust. J. Phys.* **12**: 357.

Smerd, S. F., Wild, J. P., and Sheridan, K. V. (1962).—*Aust. J. Phys.* **15**: 180.

Sturrock, P. A. (1961).—*Nature* **192**: 58.

Wild, J. P. (1962).—*J. Phys. Soc. Japan.* **17** (Suppl. A–II): 249.

Wild, J. P., Murray, J. D., and Rowe, W. C. (1954).—*Aust. J. Phys.* **7**: 439.

Wild, J. P., and Sheridan, K. V. (1958).—*Proc. Inst. Radio Engrs., N. Y.* **46**: 160.

Wild, J. P., Sheridan, K. V., and Neylan, A. A. (1959).—*Aust. J. Phys.* **12**: 369.

Wild, J. P., Sheridan, K. V., and Trent, G. H. (1959).—I.A.U.-U.R.S.I. Symposium on Radio Astronomy, Paris, 1958. p. 176. (Stanford Univ. Press.)

Appendix I

The Scatter in Position Measurements due to Non-radial Motion of the Source

The model which has been assumed is shown in Figure 7. The lobes of the interferometer lie normal to the plane of the figure. The flare position makes an angle $\frac{1}{2}\pi-\alpha$ with the interferometer scanning direction. The exciting disturbance propagates linearly through the corona, at an angle β to the flare direction. Different frequencies are assumed to originate at different fixed levels R in the corona, and refraction is neglected. R_0 is the radius of the photosphere.

The position coordinate of the burst is then

$$P = R\cos[(\tfrac{1}{2}\pi-\alpha)+\arcsin\{(R_0/R)\sin\beta\}-\beta].$$

Since $R/R_0 \sim 2$ for our frequency range, it is sufficient to use the approximation

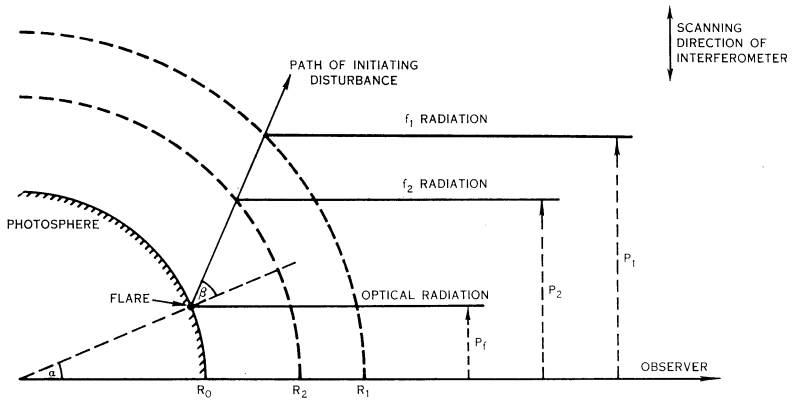

Fig. 7.—The model adopted in treating non-radial motion of the exciting disturbances of type II bursts.

$\arcsin\{(R_0/R)\sin\beta\} \sim (R_0/R)\sin\beta$. Hence

$$P = R\sin\{\alpha+\beta-(R_0/R)\sin\beta\}. \tag{1}$$

The flare position is simply

$$P_0 = R_0\sin\alpha. \tag{2}$$

If we now let β denote the semi-angle of the cone of possible directions for the exciting disturbance, the limiting burst positions are

$$P_{\text{lim}} = R\sin[\alpha\pm\{\beta-(R_0/R)\sin\beta\}], \tag{3}$$

subject to the restriction that $P = R$ for all sources beyond the radio limb. Expressions (2) and (3) define the envelopes sketched in Figure 2(*a*).

In evaluating the scatter in the variation P_1-P_2, let us first consider bursts detected at the radio limb. For such bursts either $P_1 = R_1$ or $P_2 = R_2$ and we obtain (if $P_2 = R_2$)

$$|P_1-P_2| = R_1 \cos[R_0(1/R_2-1/R_1)\sin\beta]-R_2.$$

Identifying R_1 with R_{45} and R_2 with R_{60}, and inserting numerical values from Section V, $R_0(1/R_2-1/R_1)\sin\beta<\frac{1}{8}$. Hence

$$|P_1-P_2|_1 \sim R_1-R_2,$$

and the systematic variation for limb events is independent of α and β. For bursts detected at the centre of the solar disk, let $P_1 = 0$. Then

$$|P_1-P_2|_c = P_2 = R_2 \sin[R_0(1/R_2-1/R_1)\sin\beta]$$
$$\sim R_0(1-R_2/R_1)\sin\beta.$$

Using the same numerical values as before, $|P_1-P_2|_c \sim 3'$ for $\beta = \frac{1}{2}\pi$ and $2'$ for $\beta = \frac{1}{4}\pi$.

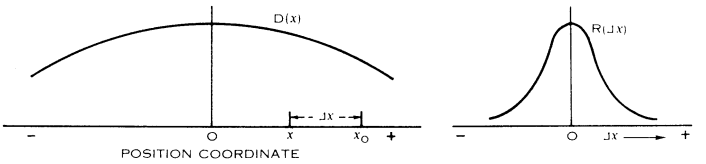

Fig. 8.—The functions $D(x)$ and $R(\Delta x)$ defined in Appendix II.

Appendix II

Errors in Position Measurements due to Irregular Ionospheric Refraction

For the purpose of evaluation of these errors, we adopt the model described in Appendix I, but with $\beta = 0$ (radial ejection). *True* burst position is then linearly related to flare position, and *true variation* (which we will term *plasma variation*) is a linear function of true burst position.

Let x denote the true position coordinate of a burst observed at x_0, both positions being reckoned in the scanning direction of the interferometer and in units of R_0. Let $x = x_0-\Delta x$. Δx, the shift of position introduced by ionospheric refraction, is a function of frequency. Further, let the true probability distribution of the position coordinates of the sources across the radio disk be $D(x)$, and let the distribution of errors in measured positions due to refraction be $R(\Delta x)$. These distributions and coordinates are illustrated schematically in Figure 8. Our object is to evaluate the total observed variation, for two unspecified frequencies f_1 and f_2 ($f_2>f_1$), in terms of the distributions $D(x)$ and $R(\Delta x)$ and the plasma variation. Since the heights of plasma levels are as yet unknown, we shall write sx for the plasma variation. s is a constant whose value is to be determined.

Δx is the shift in position for the two observing frequencies ∞ and f, say. Following Wild, Sheridan, and Neylan (1959) we shall assume that Δx is inversely proportional to the square of the frequency f. The contribution to the variation arising from ionospheric refraction, for the two frequencies f_1 and f_2, may be written as $k\Delta x$, where

$$k = f_2^2/f_1^2 - 1. \tag{4}$$

Now consider those sources, observed at x_0, whose true position is x. The total observed variation is

$$sx + k\Delta x = sx_0 + (k-s)\Delta x,$$

and the number of such sources is $D(x)R(\Delta x)\,\mathrm{d}(\Delta x)$. Hence for the distribution of the variation observed at x_0 we have

$$n[x_0,\ sx_0 + (k-s)\Delta x]\,\mathrm{d}[(k-s)\Delta x] = D(x_0 - \Delta x)R(\Delta x)\,d\Delta x. \tag{5}$$

For convenience, put $(k-s)\Delta x = y$. Then (5) becomes

$$n(x_0,\ sx_0 + y)\,\mathrm{d}y = \frac{1}{k-s} D\left(x_0 - \frac{y}{k-s}\right) R\left(\frac{y}{k-s}\right) \mathrm{d}y. \tag{6}$$

Expression (6) describes the distribution of the variation observed at x_0 as a function of the parameter y, which depends on both plasma and refraction variations. This distribution will now be evaluated for two model source distributions $D(x)$. In each case a Gaussian error distribution is assumed, that is,

$$R(\Delta x) = \exp\{-(\Delta x)^2/\sigma^2\}. \tag{7}$$

(a) Rectangular source distribution

Let

$$D(x) = 1, \qquad |x| \leqslant x_1,$$

$$= 0, \qquad |x| > x_1,$$

then

$$n(x_0,\ sx_0 + y) = 0, \qquad \begin{cases} y > (k-s)(x_0 + x_1), \\ y < (k-s)(x_0 - x_1), \end{cases}$$

$$= \{1/(k-s)\} \exp\{-y^2/(k-s)^2\sigma^2\} \text{ otherwise.} \tag{8}$$

The total number of sources observed at x_0 is

$$N = \int_{(k-s)(x_0 - x_1)}^{(k-s)(x_0 + x_1)} n(x_0,\ sx_0 + y)\,\mathrm{d}y,$$

which after some manipulation and putting $v = y/k\sigma$ becomes

$$N = \sigma \int_{a_-}^{a_+} \mathrm{e}^{-v^2}\,\mathrm{d}v. \tag{9}$$

The mean variation for given x_0 is

$$\bar{y} = \frac{1}{2N}(k-s)\,\sigma^2\,(e^{-a_-^2} - e^{-a_+^2}) \tag{10}$$

and the mean square deviation is

$$\overline{y^2} = \frac{1}{N}(k-s)^2\sigma^3 \int_{a_-}^{a_+} v^2\, e^{-v^2}\, dv - (\bar{y})^2. \tag{11}$$

In (9)–(11),

$$a_+ = \frac{x_1}{\sigma}\left(\frac{x_0}{x_1}+1\right),$$

$$a_- = \frac{x_1}{\sigma}\left(\frac{x_0}{x_1}-1\right).$$

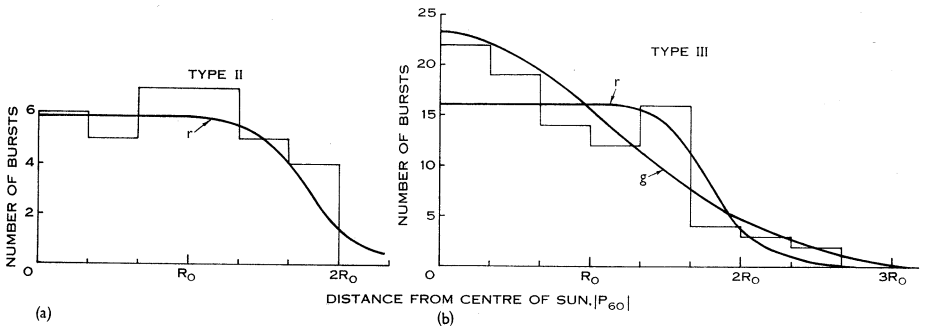

Fig. 9.—Observed distributions of sources of type II and type III bursts in the position coordinate $|P_{60}|$, compared with two predicted distributions. Details of the predicted distributions will be found in Appendix II. r is the predicted distribution derived from a rectangular probability distribution of true source position across the solar disk, and g that derived from a Gaussian source distribution.

Provided $|x_0|$ is less than, and not too close to, the value x_1, the three quantities N, $\bar{y}$, and $\overline{y^2}$ are almost independent of x_0. Then, if the whole of the observed mean square deviation of the variation from linear regression (Table 3) is attributed to irregular ionospheric refraction, an upper limit to σ can be obtained by putting $x_0 = 0$ in (11). Anticipating a later result that $x_1/\sigma \sim 4{\cdot}5$, the limits of the integration may be extended to $\pm\infty$ without appreciable error, and

$$\overline{y^2} = \tfrac{1}{2}(k-s)^2\sigma^2.$$

Putting $f_1 = 45$ and $f_2 = 60$ Mc/s gives $k = 0{\cdot}78$ from (4). Hence $\sigma^2 = 0{\cdot}05/\tfrac{1}{2}(0{\cdot}78-s)^2$. If $s = 0{\cdot}1$, $\sigma = 0{\cdot}47$; if $s = 0{\cdot}2$, $\sigma = 0{\cdot}55$. As a more reasonable value, which makes some allowance for the other causes of scatter (non-radial ejection, density fluctuations in the corona) which are surely present, we adopt $\sigma = 0{\cdot}40$.

The value of x_1 may now be estimated from the observed source distributions, by comparing them with (9). As is evident from Figure 9, the observed source distributions for both type II and type III bursts are well fitted by the theoretical curve

for $x_1 = 1{\cdot}8$. This value agrees as well as can be expected with the height of the 60 Mc/s plasma level given by the uncorrected regression coefficient (Table 3). Hence $x_1/\sigma = 4{\cdot}5$.

The parameter s now remains as the only unknown in (10), the expression for the average observed variation at x_0. This expression, with $s = 0{\cdot}20$, leads to the curves for the predicted variation which are shown in Figure 3.

(*b*) *Gaussian source distribution*

In this model, $D(x) = \mathrm{e}^{-x^2/c^2}$. Proceeding as before, we obtain

$$n(x_0, sx_0+y) = \frac{1}{k-s}\exp\left[-\frac{x_0^2}{c^2+\sigma^2}\right] \times\exp\left[-\frac{1}{(k-s)^2}\left(\frac{1}{c^2}+\frac{1}{\sigma^2}\right)\left\{y-\left(sx_0+\frac{(k-s)x_0}{1+c^2/\sigma^2}\right)\right\}^2\right]. \qquad (12)$$

The first exponential term indicates that the observed source distribution is also Gaussian, with standard deviation $(c^2+\sigma^2)^{\frac{1}{2}}/\sqrt{2}$. From the second exponential term, the average variation observed at x_0 is $\{s+(k-s)(1+c^2/\sigma^2)^{-1}\}x_0$, and the distribution of the scatter about this mean is Gaussian with a standard deviation

$$(k-s)(1/c^2+1/\sigma^2)^{-\frac{1}{2}}2^{-\frac{1}{2}}.$$

Again anticipating $c/\sigma \gg 1$, the observed error mean square deviation may be approximated by $\frac{1}{2}(k-s)^2\sigma^2$, so that $\sigma \sim 0{\cdot}40$ as before. Under this same assumption, the mean square deviation of the observed source distribution is $\sim\frac{1}{2}c^2$. As will be seen from Figure 9, the observed distribution for type III bursts can be fitted by a Gaussian curve with $c = 1{\cdot}6$, but the fit is not very convincing and the best value of c is difficult to determine. There is no justification for attempting to fit a Gaussian curve to the type II distribution. With these values for c and σ, the predicted average variation becomes $sx_0+(0{\cdot}78-s)x_0/17 = 0{\cdot}234x_0$, if $s = 0{\cdot}20$. This relation is also drawn in both parts of Figure 3.

These approximate calculations suffice to establish that the corrections to the observed variation for irregular ionospheric refraction are insensitive to the true distribution of sources on the solar disk unless $|x_0| > 2x_1$. This distribution is probably closer to rectangular than to Gaussian in form. Refraction increases the observed variation. For the frequency differential 60–45 Mc/s the amount of the increase does not exceed 20% and may be much less.

POSITIONS AND MOVEMENTS OF SOURCES OF TYPE II BURSTS

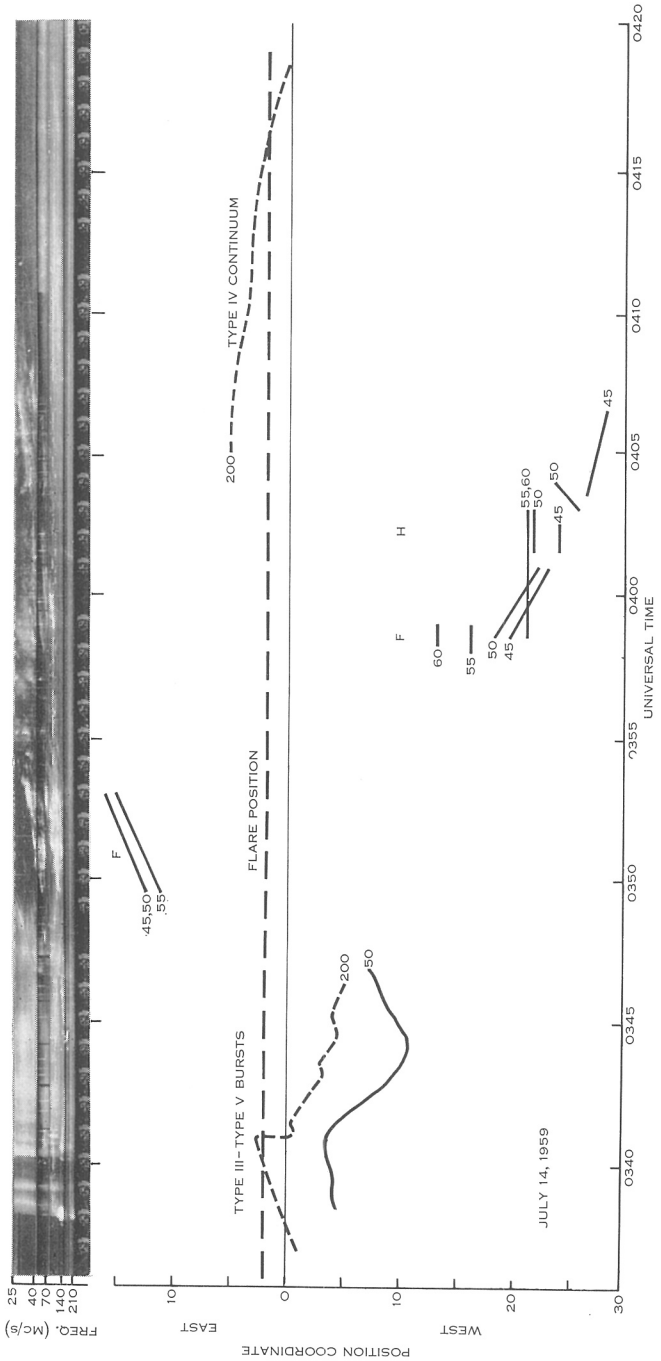

POSITIONS AND MOVEMENTS OF SOURCES OF TYPE II BURSTS

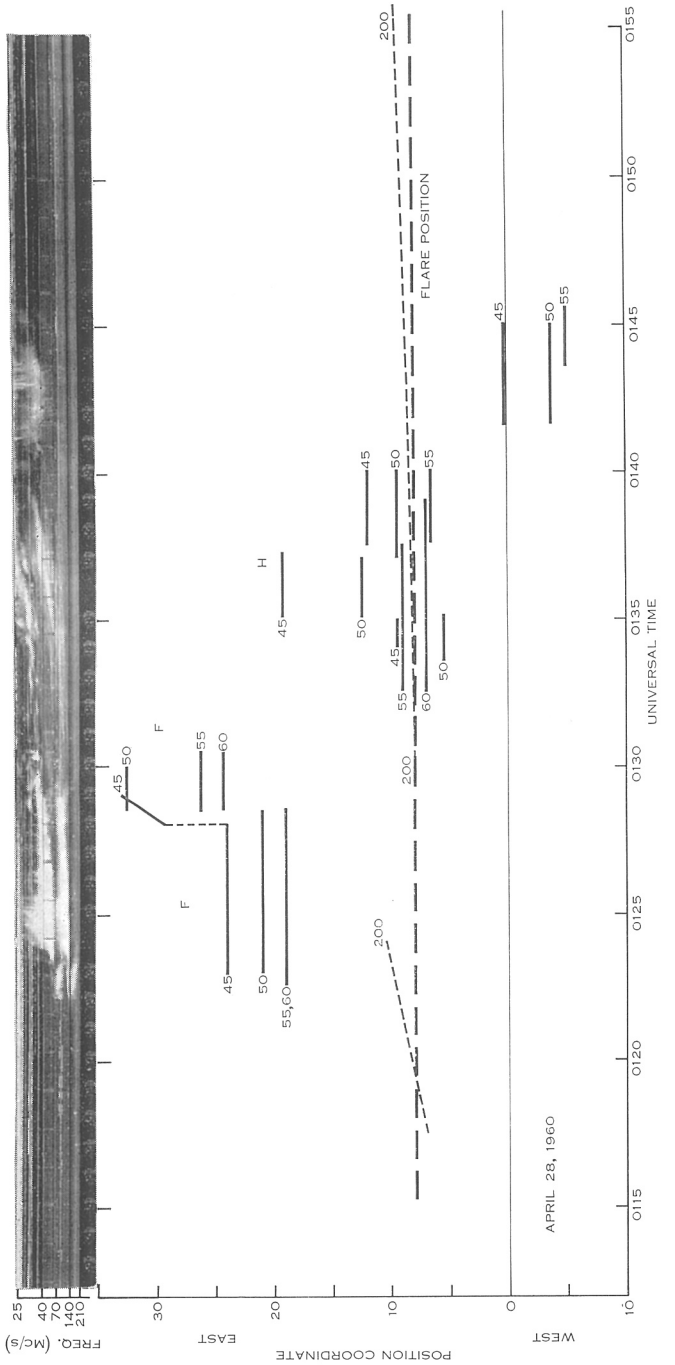

POSITIONS AND MOVEMENTS OF SOURCES OF TYPE II BURSTS

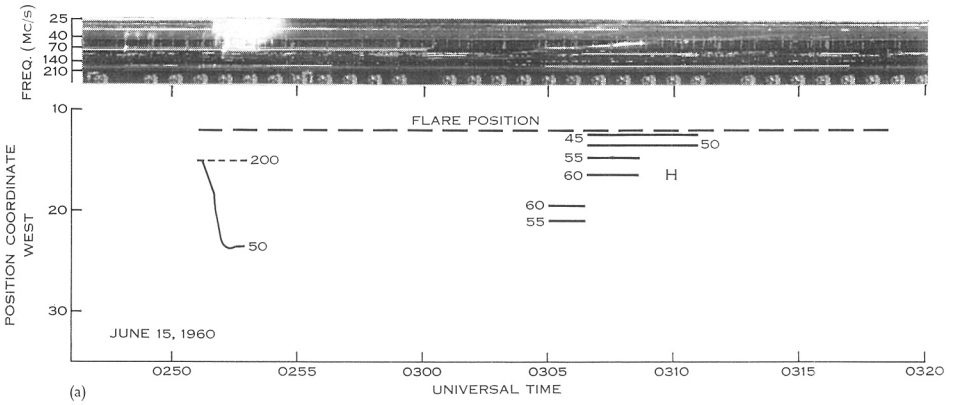

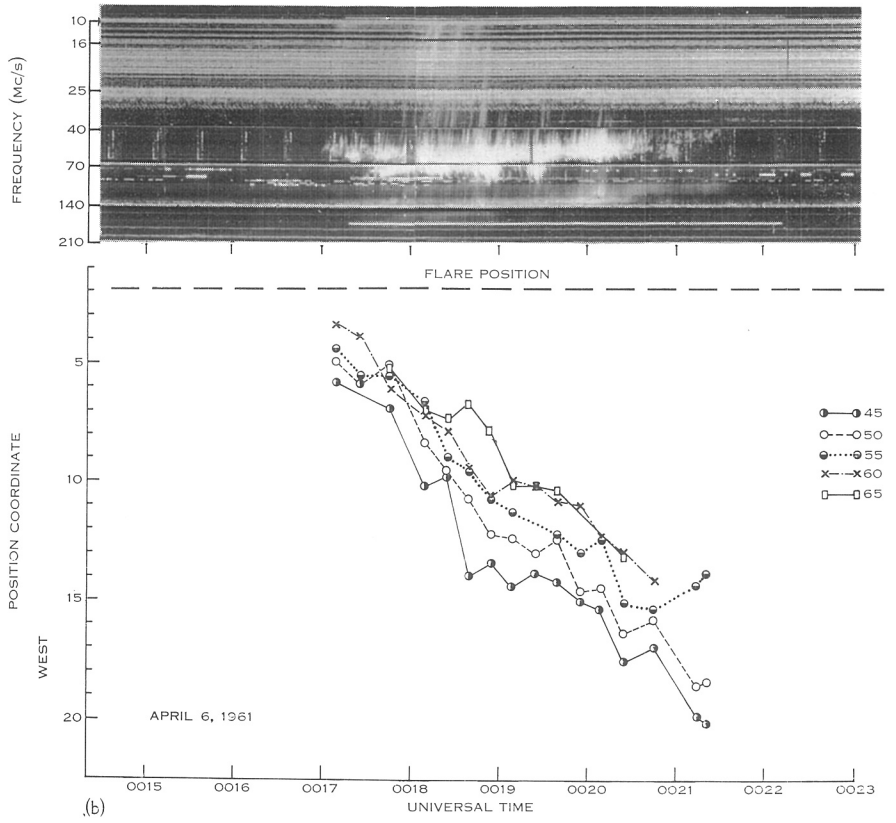

Explanation of Plates 1–3

Dynamic spectra and source positions for four type II events of special interest. The numbers against the position lines are the frequencies (in bands of 5 Mc/s width) at which the measurements were made. The symbols F and H refer to the harmonic structure of the bands (F = fundamental band, H = second harmonic band).

Plate 1

July 14, 1959. The event appears to consist of two type III–type II compound bursts, followed by a type IV continuum whose position was not measured in the 45–60 Mc/s frequency range. The two exciting disturbances of the type II bursts seem to have been ejected into opposite hemispheres of the Sun; this may be linked with two loop-shaped flare brightenings, one pointing eastwards and the other westwards. The temporal changes in position of each of the sources of the type II bursts could be continuations of the changes in position of the sources of the type V bursts which are evident at both 200 Mc/s and 50 Mc/s. It is suggested that such movements at a single frequency are indicative of a tangential component in the motion of the exciting disturbance. The abrupt increase in spectral intensity in the 40–70 Mc/s range shortly after 0410 U.T. marks the time when the interferometer was switched off.

Plate 2

April 28, 1960. The most complex event encountered during the present study. It illustrates the need for elaborate observations in sorting out the more complex type II events. The whole event is seen to consist of at least three separate bursts. The positions of the three features which appear to comprise the main burst in the 40–70 Mc/s range (fundamental band 0122–0129 U.T., second harmonic band 0132–0140 U.T., irregular continuum 0141–0145 U.T.) are displaced successively westwards, but there is no evidence for any apparent tangential motion of the source *within* each feature. The minor bursts, 0128–0131 U.T. and 0135–0138 U.T., have source positions differing from those of the main burst; the spectrum of the second of these is also characterized by a frequency drift rate about three times as large as for the main burst. The irregular continuum which terminates the event has been classified as a type II burst since it exhibits the normal systematic variation of position with frequency and also has a source brightness distribution typical of the sources of type II bursts. The flare which gave rise to this event was also very complex, with two parallel open loops and numerous bright knots. Attempts to link radio and optical features were unsuccessful.

Plate 3

(*a*) *June 15, 1960.* This is a further example of a multiple burst with two sources in different positions and with different frequency drift rates. The spectrum also illustrates the low intensity and poor definition of fundamental bands which are characteristic of type II bursts associated with flares near the optical limb.

(*b*) *April 6, 1961.* The spectrum of this burst shows the low frequency drift rate which has been noted as characteristic of the class of bursts whose source positions change with time at constant frequency. The individual position measurements, plotted in five frequency bands, leave little doubt that in the case of this burst the apparent movement of the source cannot be attributed to ionospheric refraction.